

GFP-'Walking': Artificial Construct Aberrations

Caused by Cotransfectional Homologous Recombination



Felix Bestvater

Eberhard Spiess

Biomedical Structure Analysis

Tobias A. Knoch

Jörg Langowski

Biophysics of Macromolecules

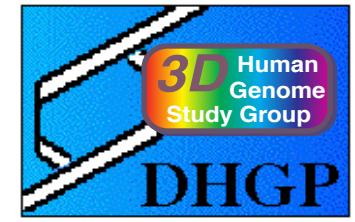
German Cancer Research Center (DKFZ)

Heidelberg - Germany

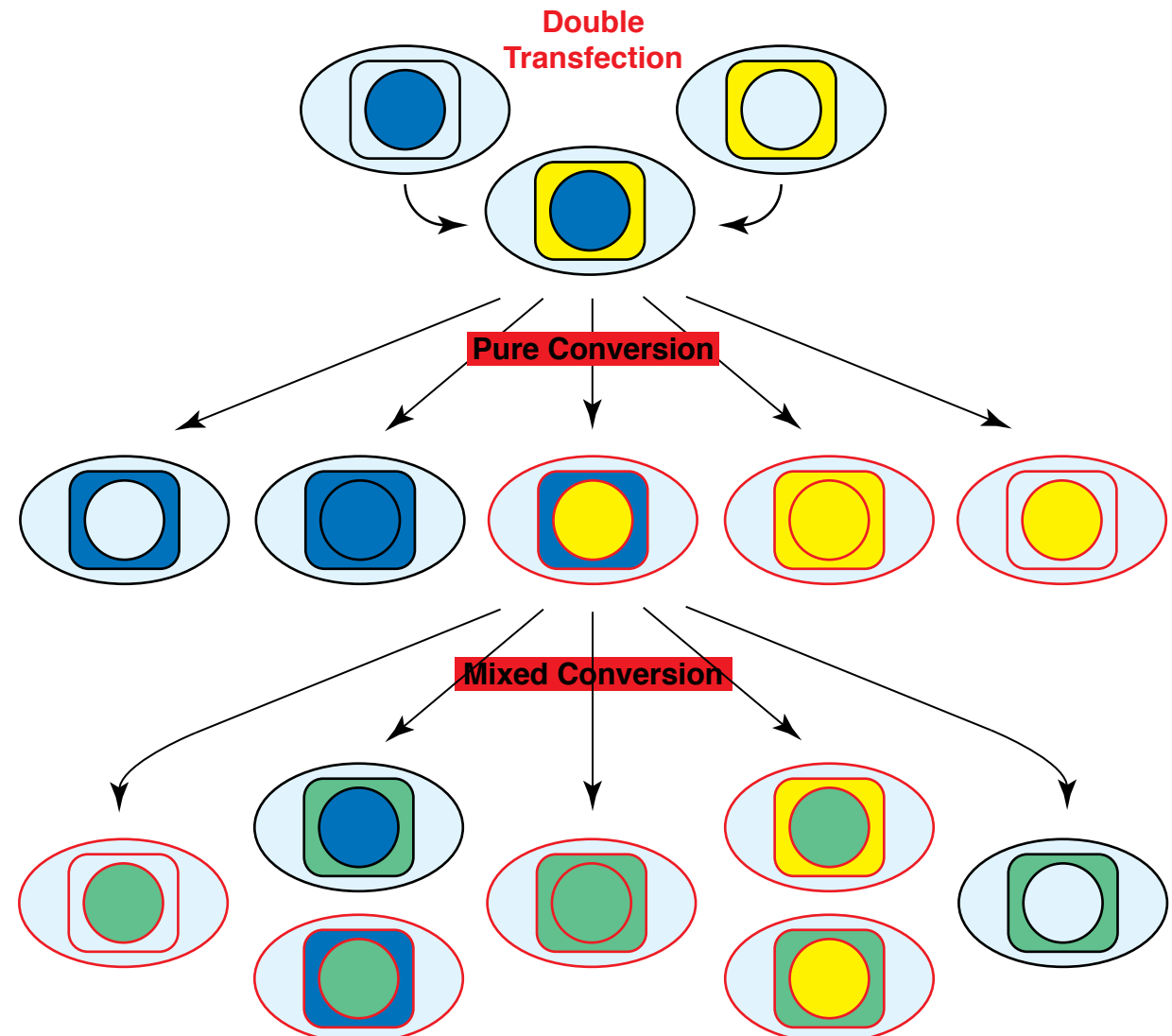
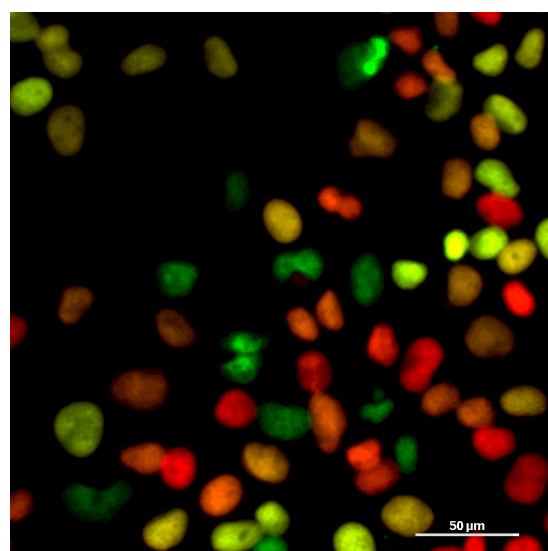
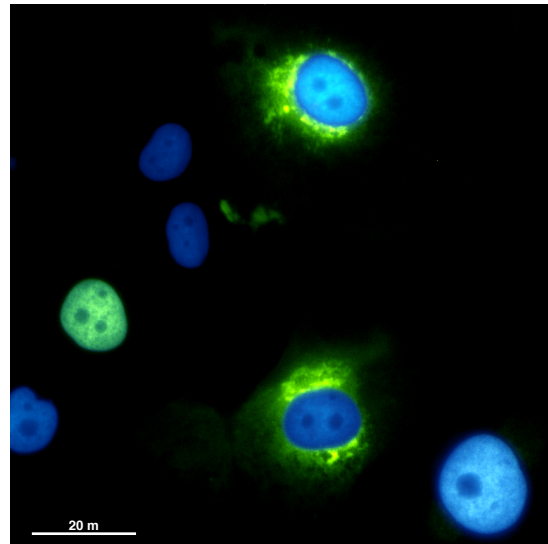
Simultaneous cotransfection of GFP-chimeras lead to a GFP conversion:

All conversion possibilities were observed by cotransfected H2A-CFP (SV40, strong expression, localized in the nucleus) and CB-YFP (CMV, weak expression, localized in the ER/Golgi).

The convertants can be enriched and stable cell lines can be created.

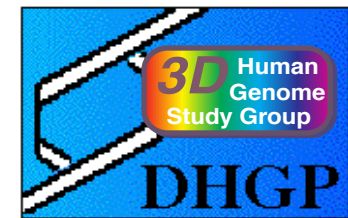


Tobias A. Knoch



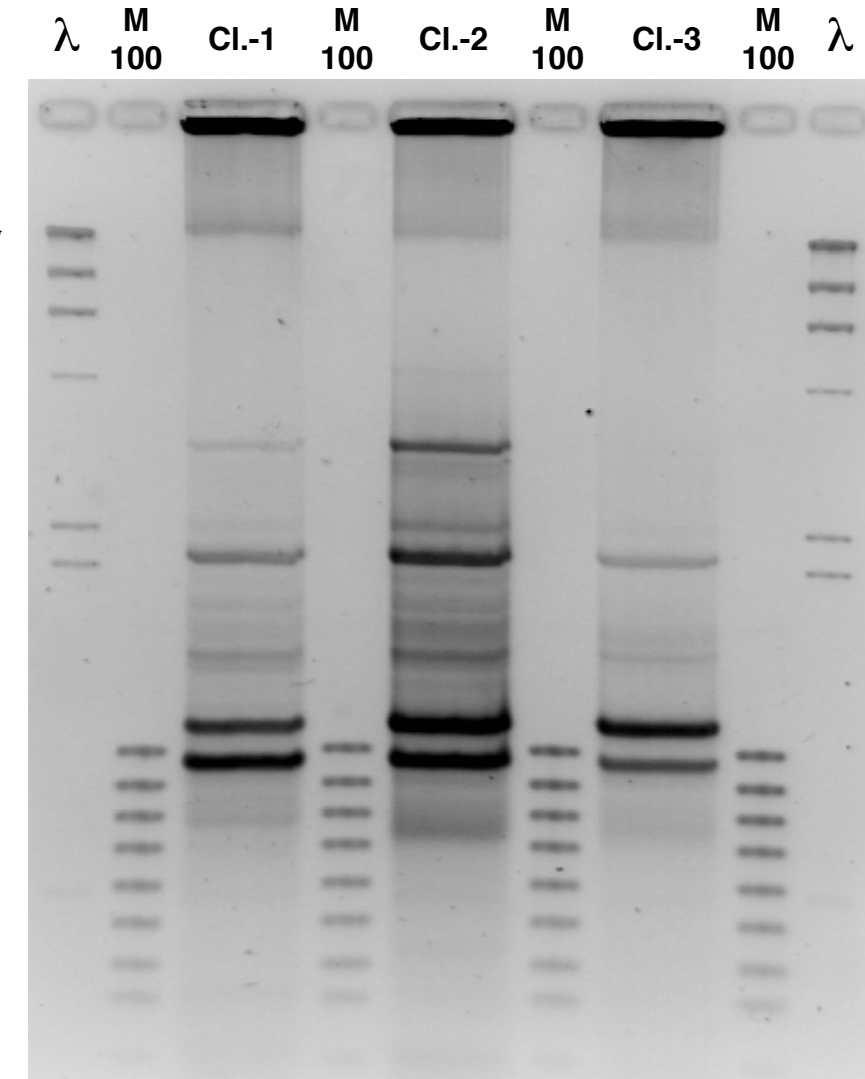
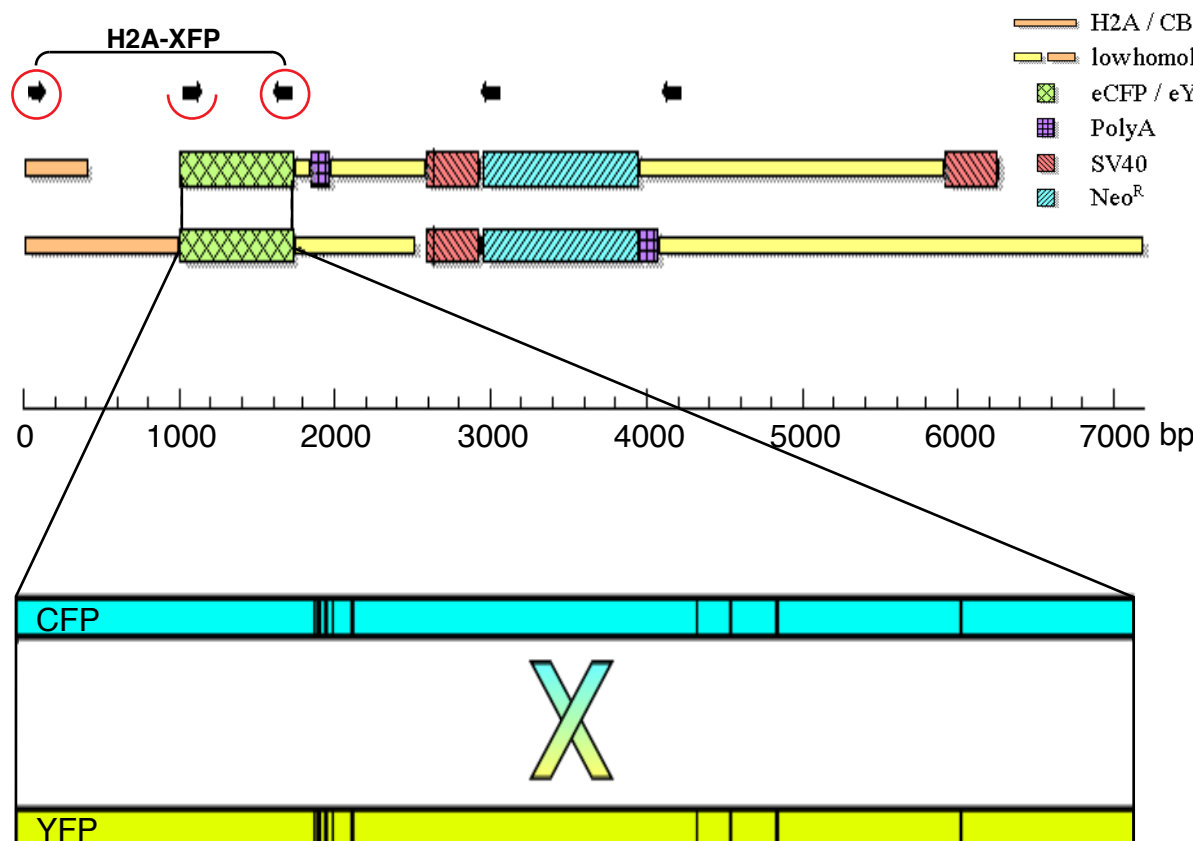
Homology analysis of vectors and genomic PCR for proof of conversion:

A homology analysis of H2A-CFP and CB-YFP suggests homologous recombination as cause of conversion.
The final proof of conversion was obtained with a genomic PCR of the full H2A-XFP fusion gene and sequencing of the PCR.



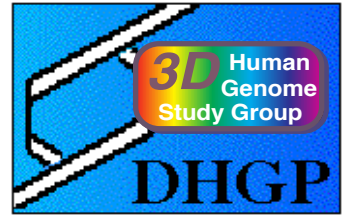
Tobias A. Knoch

Homology Comparison of H2A-CFP and CB-YFP



2% Agarose Gel, 40V, 4C, 20cm

Final proof of the conversion events by analysis of the sequenced PCR of an conversion enriched cell clone: The conversion takes place in all 16 bp mutations separating CFP and YFP .



Tobias A. Knoch

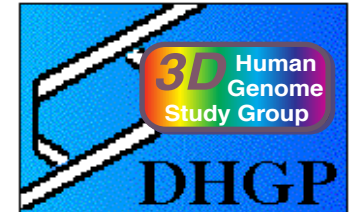
H2A-ECFP	GGGATCCACCGTCGCCACC	ATGGT GAGCAAGGGCAGGAGCTGTT	CACC
H2A-YFP (Cl.1)	GGGATCCACCGTCGCCACC	ATGGT GAGCAAGGGCAGGAGCTGTT	CACC
eYFP	-----	ATGGT GAGCAAGGGCAGGAGCTGTT	CACC
H2A-ECFP	GGGGTGGTGCCCATCCTGGTC	GAGCTGGACGGG	GACGTAAACGGCCACAA
H2A-YFP (Cl.1)	GGGGTGGTGCCCATCCTGGTC	GAGCTGGACGGG	GACGTAAACGGCCACAA
eYFP	GGGGTGGTGCCCATCCTGGTC	GAGCTGGACGGG	GACGTAAACGGCCACAA
H2A-ECFP	GTTCAGCGTGTCCGGCGAGGGCGAGGGCGA	GCCACCTACGG	CAAGCTGA
H2A-YFP (Cl.1)	GTTCAGCGTGTCCGGCGAGGGCGAGGGCGA	GATGCCACCTACGG	CAAGCTGA
eYFP	GTTCAGCGTGTCCGGCGAGGGCGAGGGCGA	GATGCCACCTACGG	CAAGCTGA
H2A-ECFP	CCCTGAAGTTCATCTGCACCACCGG	CAAGCTGCC	GCTGCCCTGGCCCACC
H2A-YFP (Cl.1)	CCCTGAAGTTCATCTGCACCACCGG	CAAGCTGCC	GCTGCCCTGGCCCACC
eYFP	CCCTGAAGTTCATCTGCACCACCGG	CAAGCTGCC	GCTGCCCTGGCCCACC
H2A-ECFP	CTCGTGACCACCC	CTGACCTGGGCGTGCAGTGCTTCAGCC	GCTACCCCGA
H2A-YFP (Cl.1)	CTCGTGACCACCT	tTcgGCTacGGC	tCCGCTACCCCGA
eYFP	CTCGTGACCACCT	tTcgGCTacGGC	tCCGCTACCCCGA
H2A-ECFP	CCACATGAAGCAGCACGACTT	CTTCAGTCCGCC	ATGCCGAAGGCTACG
H2A-YFP (Cl.1)	CCACATGAAGCAGCACGACTT	CTTCAGTCCGCC	ATGCCGAAGGCTACG
eYFP	CCACATGAAGCAGCACGACTT	CTTCAGTCCGCC	ATGCCGAAGGCTACG
H2A-ECFP	TCCAGGAGCGCACC	ATCTTCAGGACG	ACGGCAACTACAAGACCCGC
H2A-YFP (Cl.1)	TCCAGGAGCGCACC	ATCTTCAGGACG	ACGGCAACTACAAGACCCGC
eYFP	TCCAGGAGCGCACC	ATCTTCAGGACG	ACGGCAACTACAAGACCCGC
H2A-ECFP	GCCGAGGTGAAGTT	CGAGGGCGACACC	CTGGTAACCGCATCGAGCTGAA
H2A-YFP (Cl.1)	GCCGAGGTGAAGTT	CGAGGGCGACACC	CTGGTAACCGCATCGAGCTGAA
eYFP	GCCGAGGTGAAGTT	CGAGGGCGACACC	CTGGTAACCGCATCGAGCTGAA
H2A-ECFP	GGGCATCGACTT	CAAGGAGGACGG	CAACATCCTGGG
H2A-YFP (Cl.1)	GGGCATCGACTT	CAAGGAGGACGG	CAACATCCTGGG
eYFP	GGGCATCGACTT	CAAGGAGGACGG	CAACATCCTGGG
H2A-ECFP	ACAACTACAT	CAGCCACAACG	TCTATATCACCG
H2A-YFP (Cl.1)	ACAACTACAA	CAGCCACAACG	TCTATATCACG
eYFP	ACAACTACAA	CAGCCACAACG	TCTATATCACG
H2A-ECFP	GGCATCAAGGCC	AACTTCAAGA	TCCGCCACAACATCGAGG
H2A-YFP (Cl.1)	GGCATCAAGGt	tgAACTTCAAGA	TCCGCCACAACATCGAGG
eYFP	GGCATCAAGGt	tgAACTTCAAGA	TCCGCCACAACATCGAGG
H2A-ECFP	GCAGCTCGCC	GACCACTACCAG	CAGAGACACCCCC
H2A-YFP (Cl.1)	GCAGCTCGCC	GACCACTACCAG	CAGAGACACCCCC
eYFP	GCAGCTCGCC	GACCACTACCAG	CAGAGACACCCCC
H2A-ECFP	TGCTGCTGCCG	GACAACCACTAC	CTGAGCACCC
H2A-YFP (Cl.1)	TGCTGCTGCCG	GACAACCACTAC	CTGAGCACCC
eYFP	TGCTGCTGCCG	GACAACCACTAC	CTGAGCACCC
H2A-ECFP	GACCCCAACG	GAGAAGCG	GATCACATGG
H2A-YFP (Cl.1)	GACCCCAACG	GAGAAGCG	GATCACATGG
eYFP	GACCCCAACG	GAGAAGCG	GATCACATGG
H2A-ECFP	CGCCGGGATC	ACTCTCGG	CATGGGACGAGCTGTACAAGTAA
H2A-YFP (Cl.1)	CGCCGGGATC	ACTCTCGG	CATGGGACGAGCTGTACAAGTAA
eYFP	CGCCGGGATC	ACTCTCGG	CATGGGACGAGCTGTACAAGTAA

Quantifying the conversion rate:

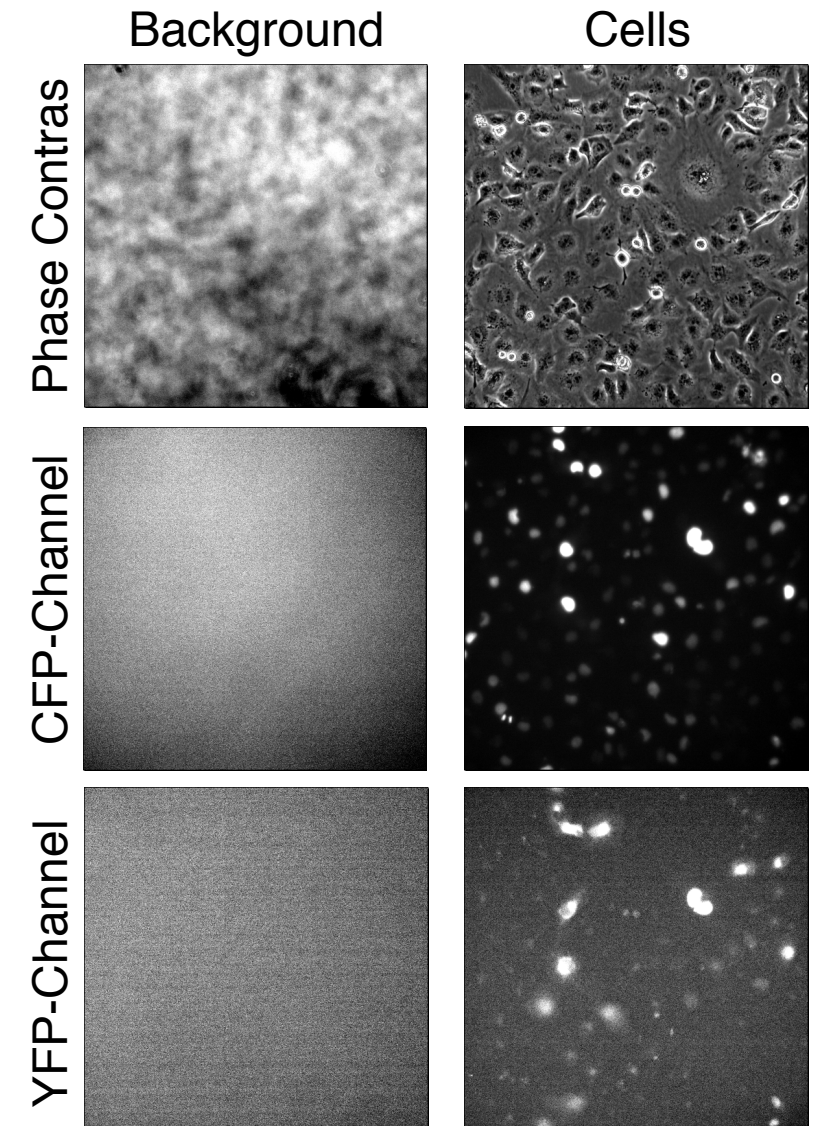
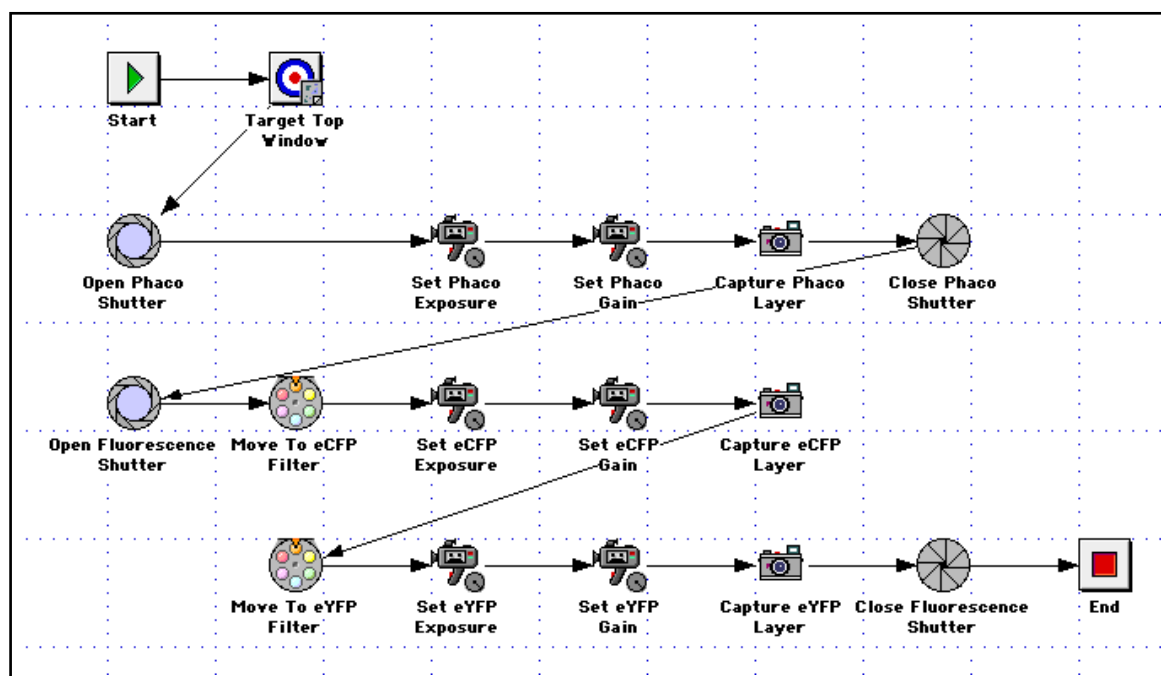
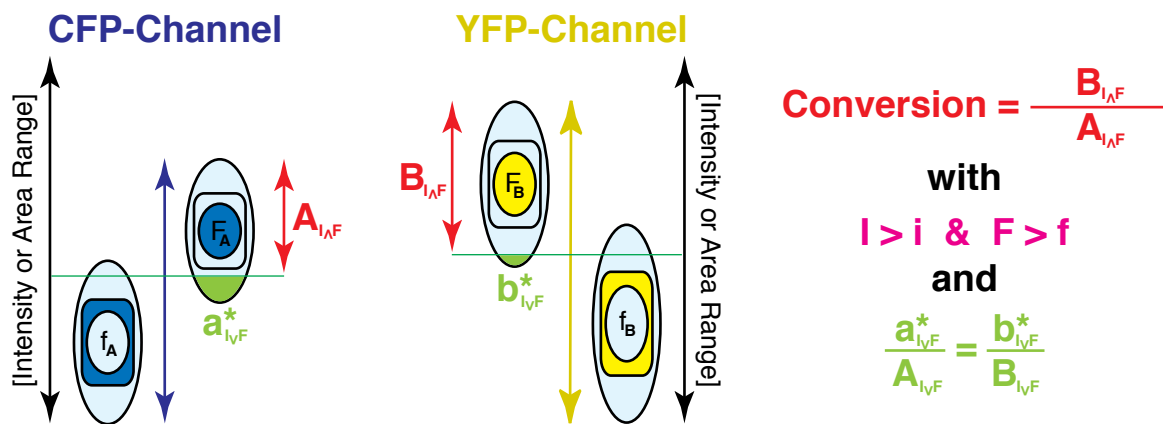
For quantifying the conversion rate images were taken in the phase contrast-, CFP- and YFP- channel with a Zeiss Axiovert S100 TV.

The image acquisition can partly be automated with macros.

Reliable conversion rates critically depend on many a parameter!

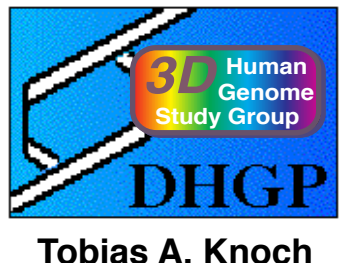


Tobias A. Knoch



Quantifiing the conversion - Image Aquisition:

For quantifiing the conversion rate images were taken in the phase contrast-, CFP- and YFP- channel with a Zeiss Axiovert S100 TV.

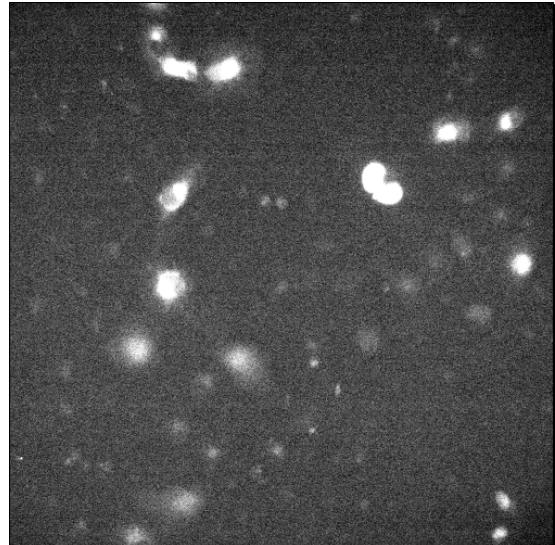
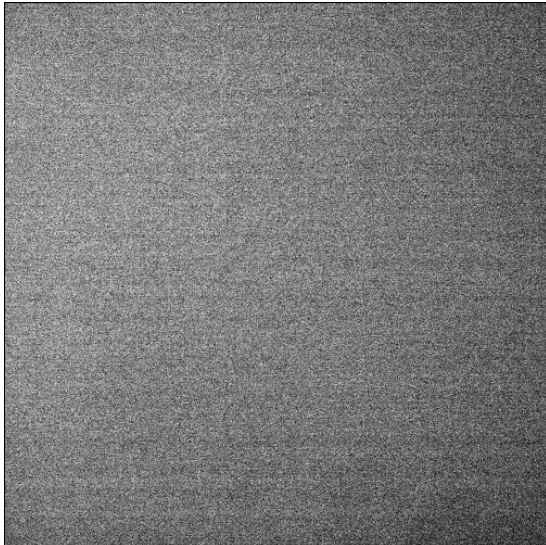
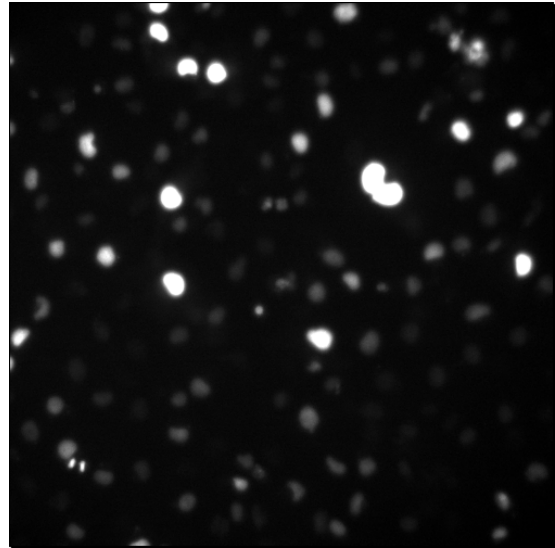
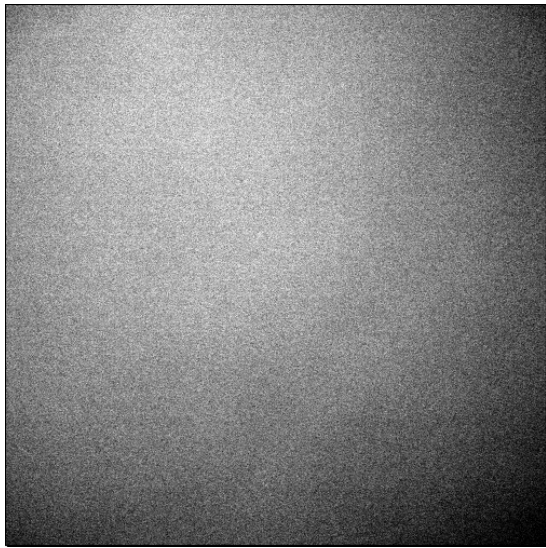
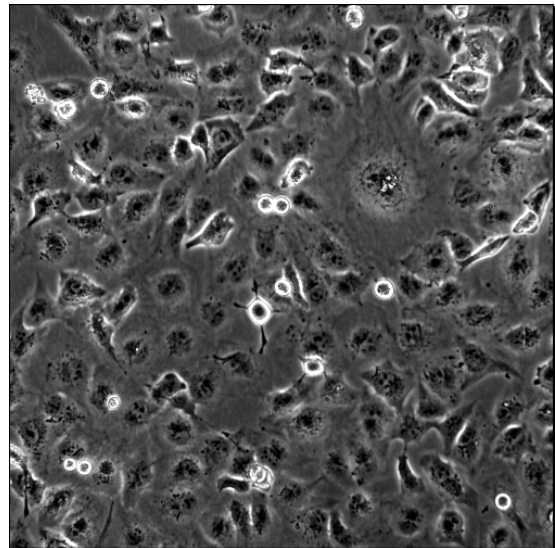
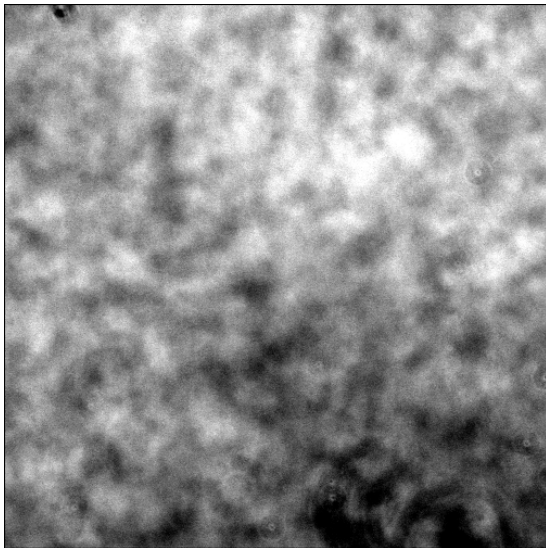


Background
Cells

Phase Contrast

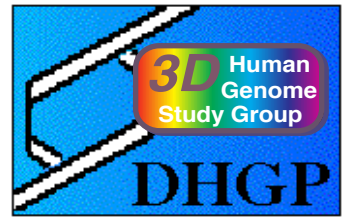
CFP-Channel

YFP-Channel

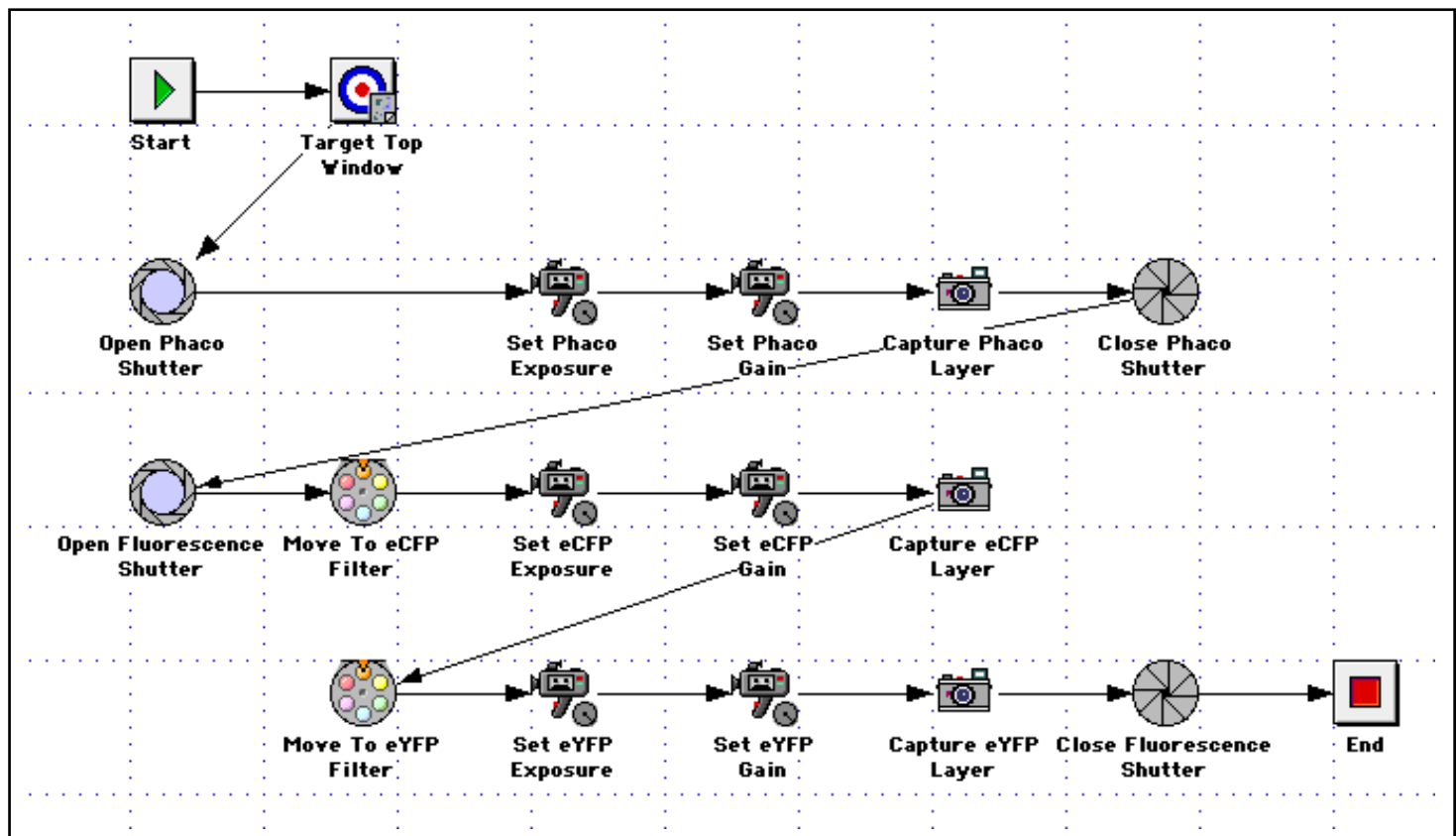


Quantifying the conversion - Image Aquisition:

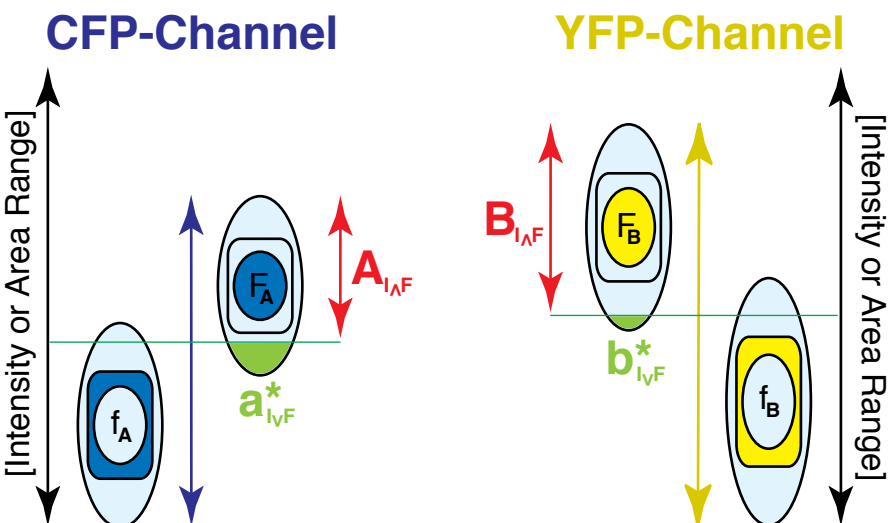
Although the image taking can partly be automated by macros, a reliable conversion rate depends critically on the aquisition parameters as well as on the vector system !



Tobias A. Knoch

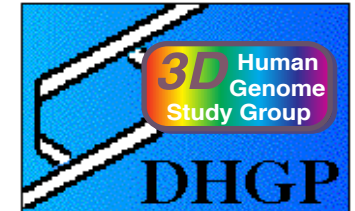


$$\text{Conversion} = \frac{B_{I_{AF}}}{A_{I_{AF}}} \quad \text{with} \quad I > i \quad \& \quad F > f \quad \text{and} \quad \frac{a^*_{I_{yF}}}{A_{I_{yF}}} = \frac{b^*_{I_{yF}}}{B_{I_{yF}}}$$

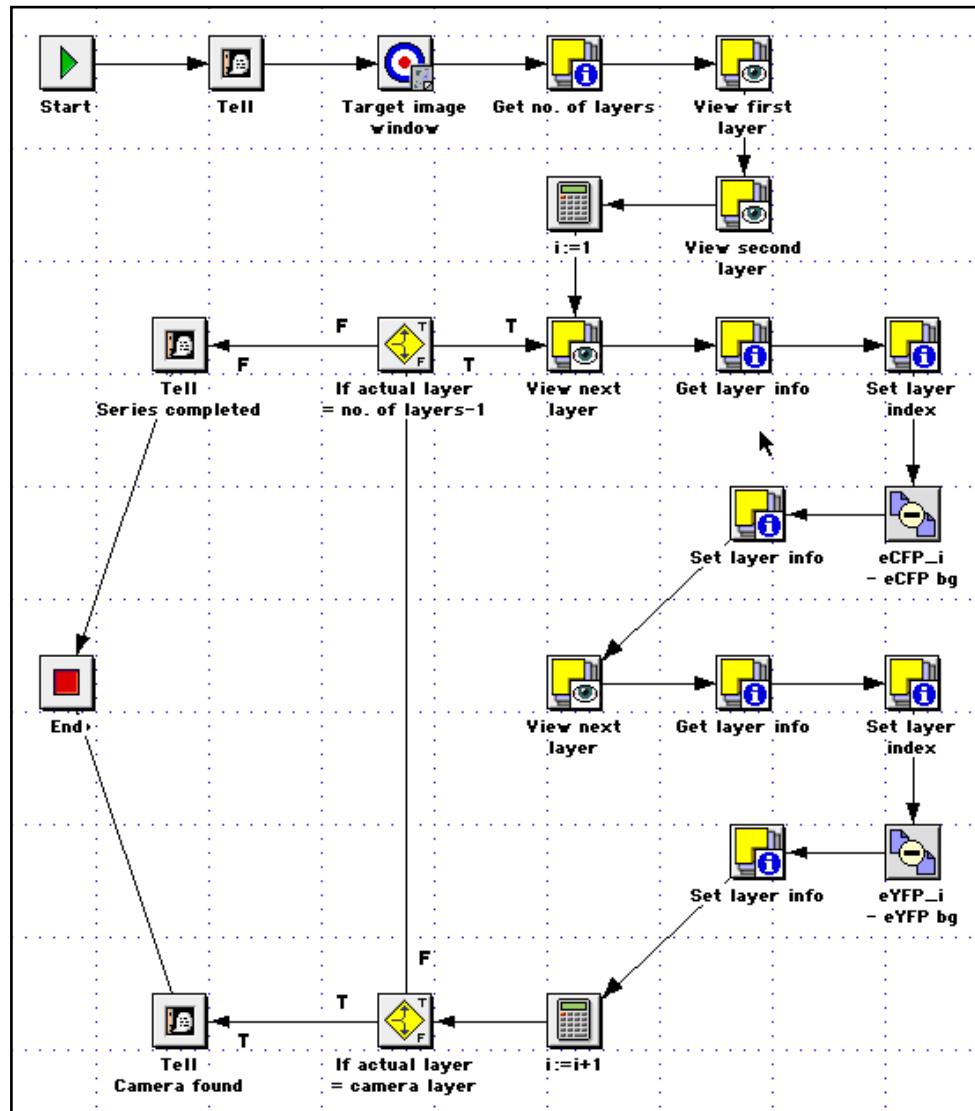


Quantifying the conversion - Numeration and Background Subtraction:

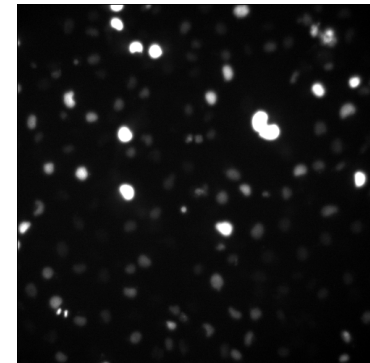
For later digital image processing the images have to be numbered and the background having no isotrope distribution accross the field of illumination is subtracted using again a macro.



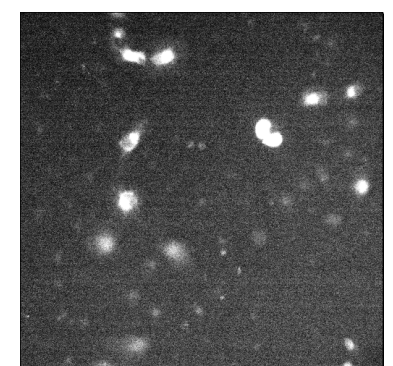
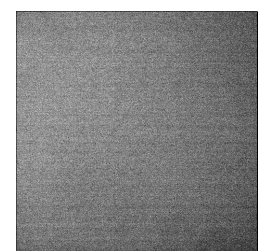
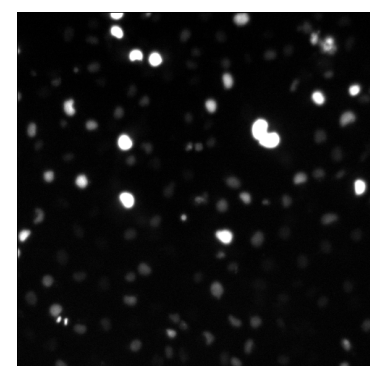
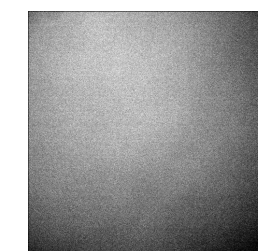
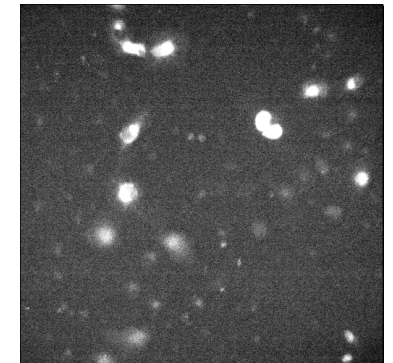
Tobias A. Knoch



CFP-Channel



YFP-Channel

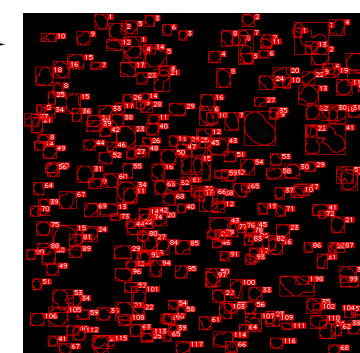
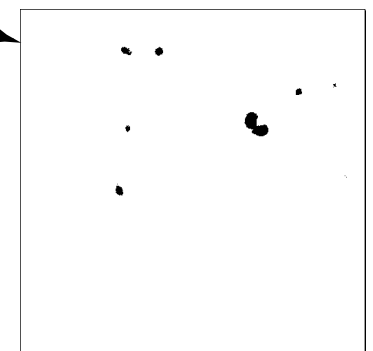
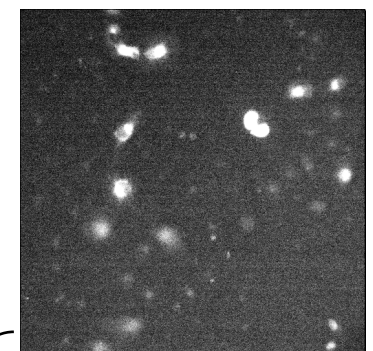
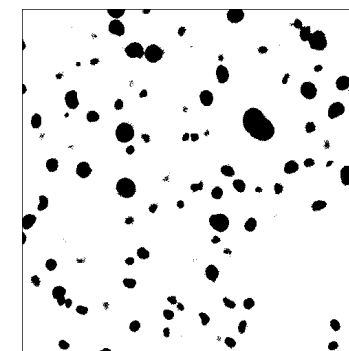
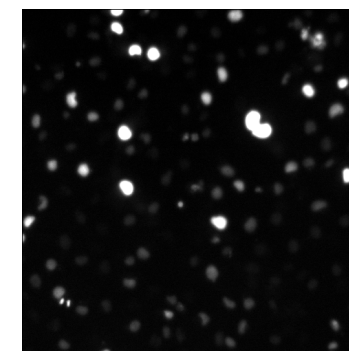
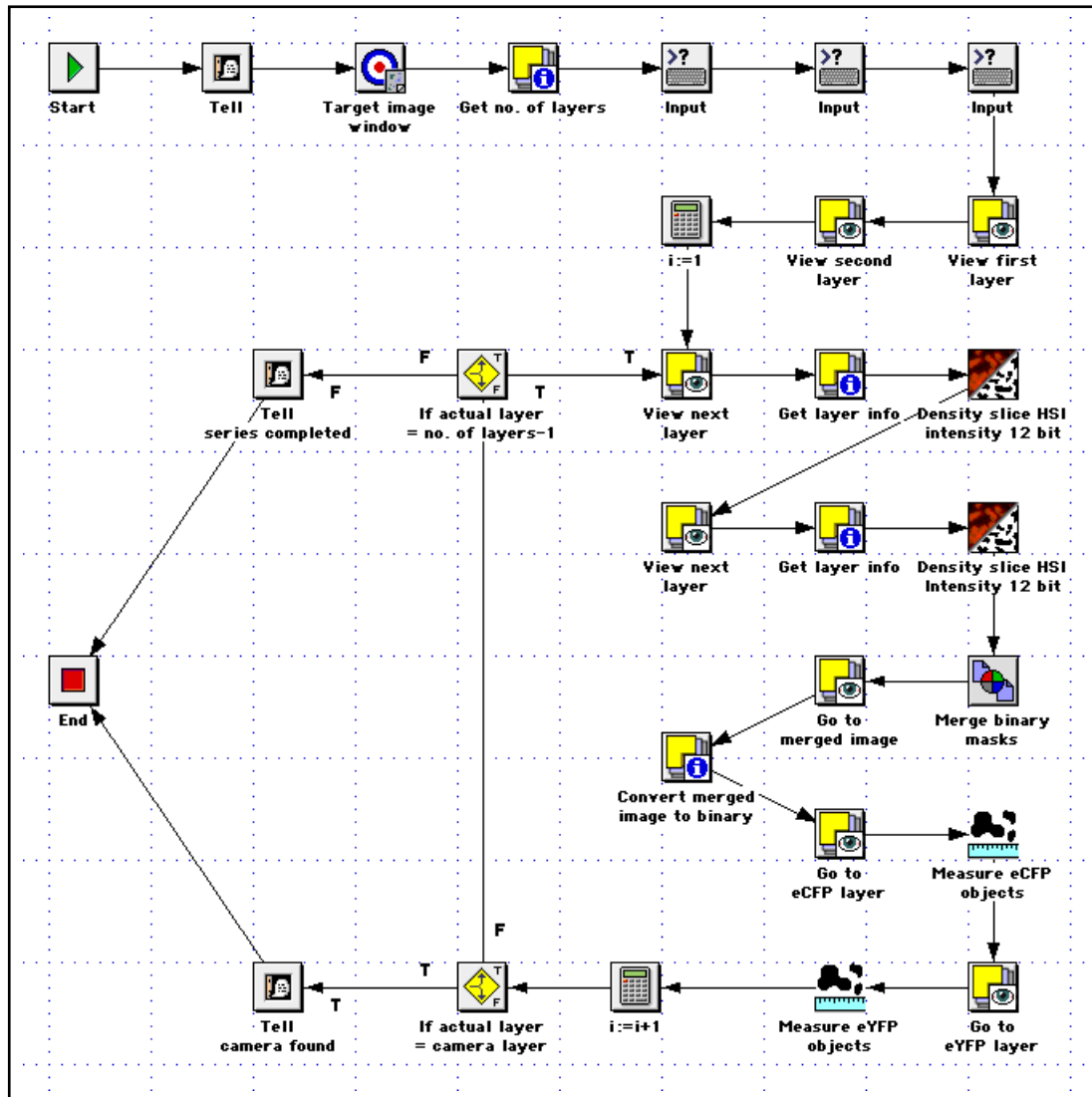


Quantifying the conversion - Signal Analysis:

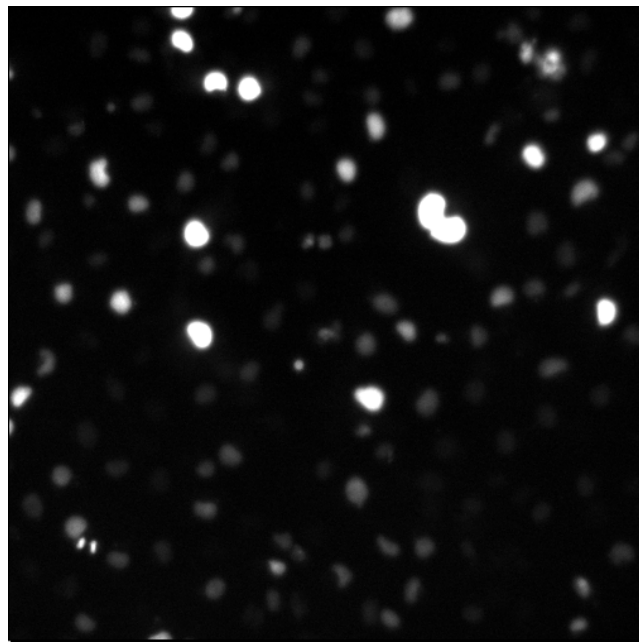
With intensity thresholds, binary masks of each channel are created separating most H2A from CB signals. With the merged binary masks the signals in each channel are reevaluated, followed by an area separation of the H2A from the CB signal. The data can be checked in a result image.



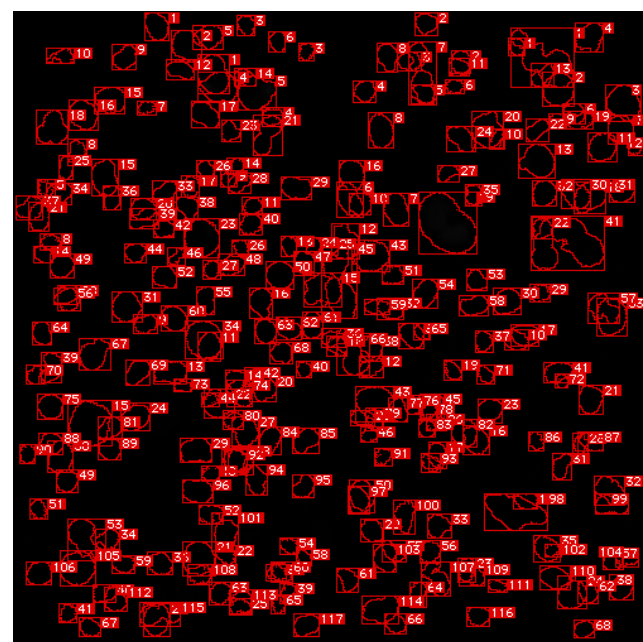
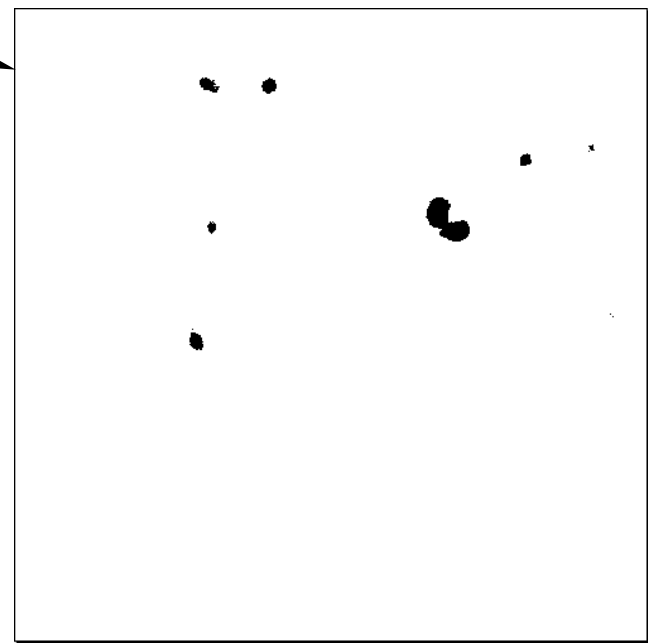
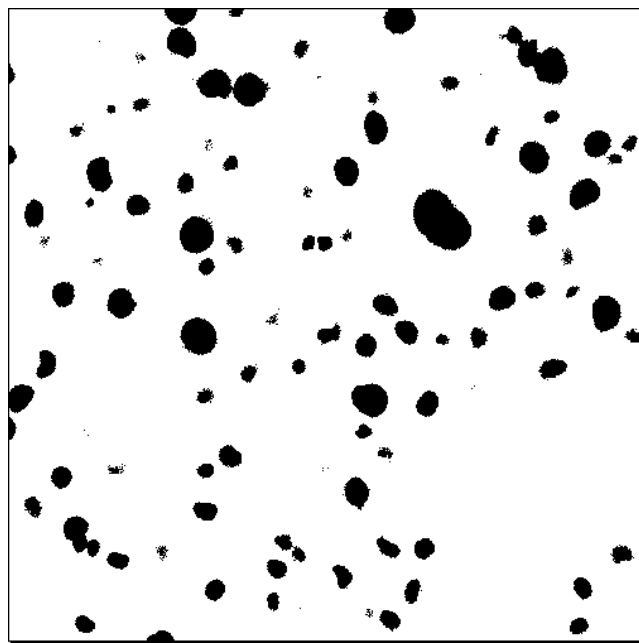
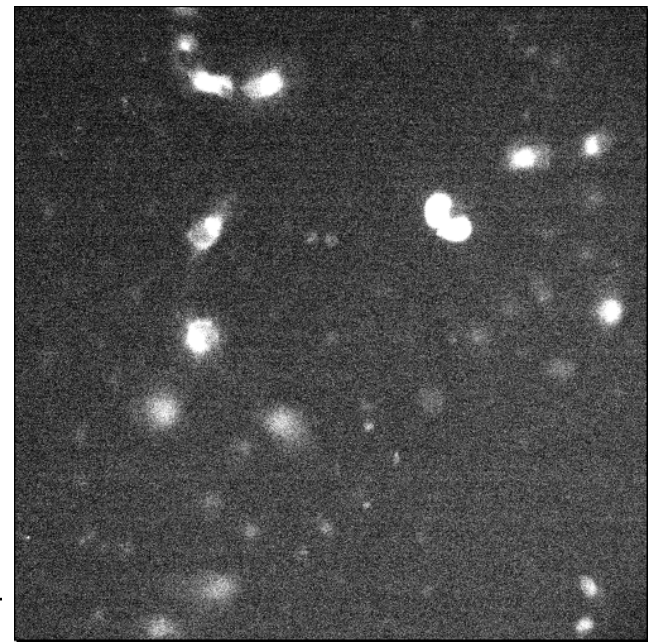
Tobias A. Knoch



CFP-Channel



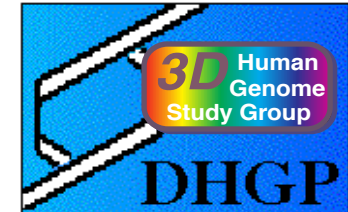
YFP-Channel



Various conversion experiments proof the high rate of conversion:

For sufficient statistics in each experiment 1000 to 3000 signals were obtained, including tests totaling to more than 50.000.

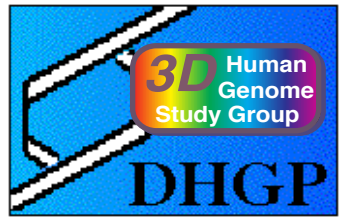
In general conversion appears with different vectors, cell lines, and methods of transfection, but not in overtransfection of a stable cell line !



Tobias A. Knoch

Construct	Cells	Method		Conversion [+/-] and [%]
H2A-CFP	LCLC103H	FuGene6		- 0.0
CB-YFP	LCLC103H	FuGene6		- 0.0
H2A-CFP + CB-YFP	LCLC103H	FuGene6	simultanious	+ 4.0 0.2
H2A-CFP + DsRed	LCLC103H	FuGene6	simultanious	- 0.0
H2A-CFP + pure GFP	LCLC103H	FuGene6	simultanious	+ >1.0
H2A-CFP + CB-YFP	LCLC103H	FuGene6	sep. Mix + simultanious	+ >1.0
H2A-CFP + CB-YFP	LCLC103H	FuGene6	sep. Mix + 4 h delay	- (+) 0.0 (7.3)
H2A-CFP* + CB-YFP	LCLC103H	FuGene6	overtransfec. *stable line	- 0.0
H2A-CFP + CB-YFP	LCLC103H	FuGene6	5x DNA conc	+ ?
H2A-CFP + CB-YFP	LCLC103H	FuGene6	10x DNA conc	+ ?
H2A-CFP + CB-YFP	LCLC103H	FuGene6	linearized	+ 3.4
H2A-CFP + CB-YFP	LCLC103H	FuGene6	linearized + 96C	+++ 10.3
H2A-CFP + CB-YFP	LCLC103H	Dmrie-C	simultanious	+ 3.8
H2A-CFP + CB-YFP	LCLC103H	Cellfectin	simultanious	+ >1.0
H2A-CFP + CB-YFP	LCLC103H	Lipofectin	simultanious	+ 2.4
H2A-CFP + CB-YFP	LCLC103H	GibcoPlus	simultanious	+ >1.0
H2A-CFP + CB-YFP	LCLC103H	Electroporation	simultanious	+ ~1.0
H2A-CFP + CB-YFP	LCLC103H	Ca-Phosphat	simultanious	+ ~1.0
H2A-CFP	HeLa	FuGene6		- 0.0
H2A-CFP + CB-YFP	HeLa	FuGene6	simultanious	+ ?
H2A-CFP	Cos-7	FuGene6		- 0.0
H2A-CFP + CB-YFP	Cos-7	FuGene6	simultanious	+ ?

Summary and Outlook



Tobias A. Knoch

Warning

simultaneous cotransfections can lead to GFP-walking

**the artificial and misleading results due to conversion
are usually between 2% and 8%
and can reach up to ~20% in the extrem**

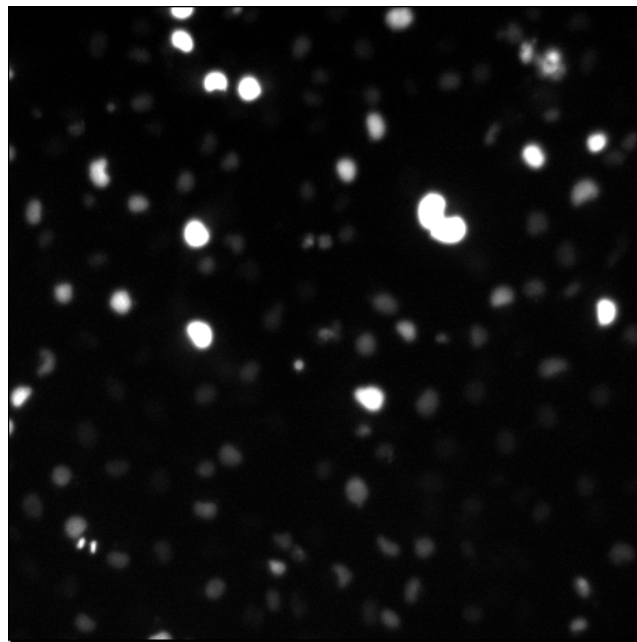
**the conversion can be reduced dramatically
by successive transfection
and overtransfection of a stably transfected cell line**

Application

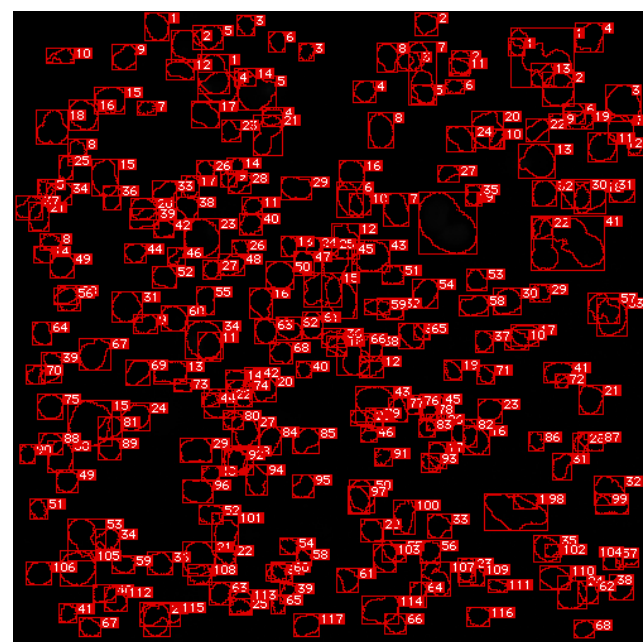
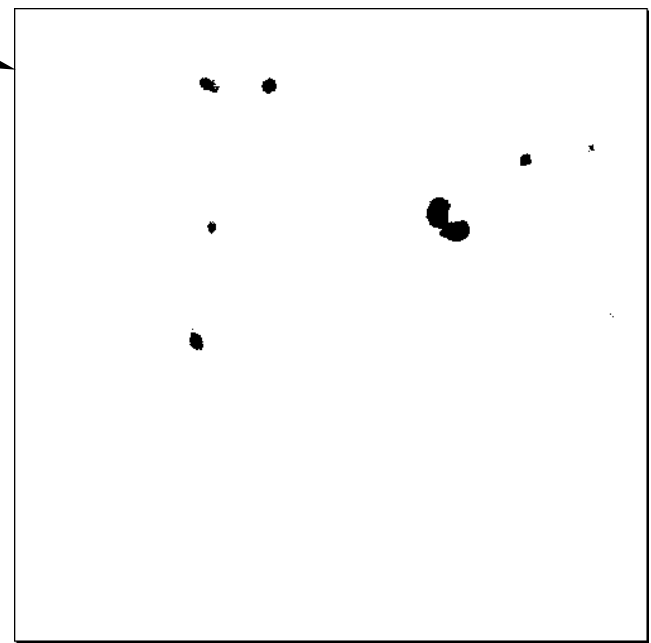
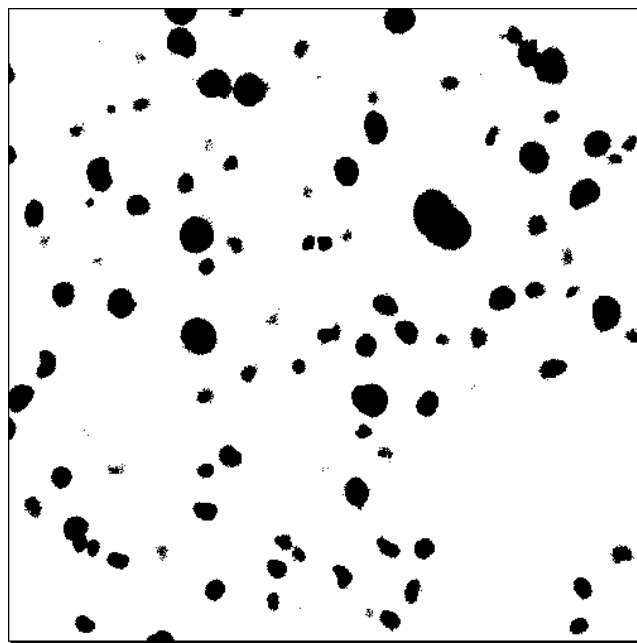
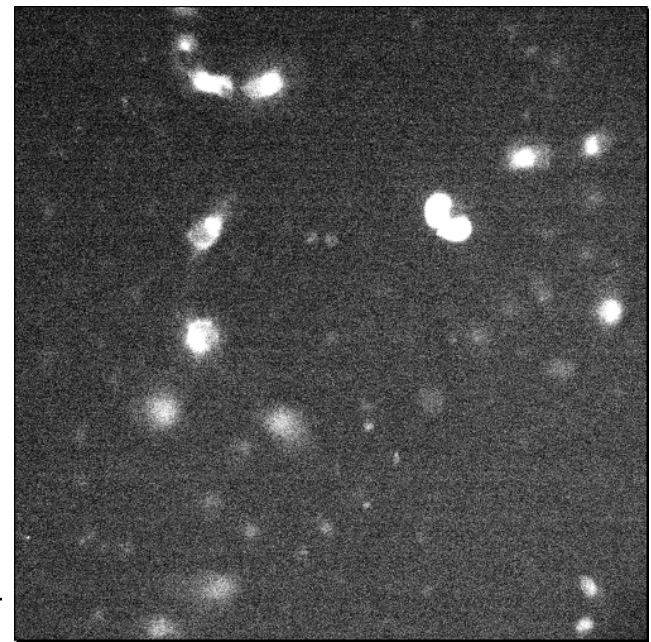
**a fast method for expressing a fusion protein with
another GFP without creating a new DNA plasmid
and receiving immediately a clone of a cell line**

**this system is a suitable tool for the investigation
of homologous recombination
(e.g. cancer cells with elevated recombination activity)
or similar processes
(an optimized system for FACS analysis is possible)**

CFP-Channel



YFP-Channel



“GFP-Walking”: Artificial Construct Aberrations caused by Co-Transfectional Homologous Recombination

Knoch, T. A.

*Biophysics of Macromolecules Seminar, German Cancer Research Centre (DKFZ),
Heidelberg, Germany, July, 2000.*

Corresponding author email contact: TA.Knoch@taknoch.org

Keywords:

Genome, genomics, genome organization, genome architecture, structural sequencing, architectural sequencing, systems genomics, coevolution, holistic genetics, genome mechanics, genome function, genetics, gene regulation, replication, transcription, repair, homologous recombination, simultaneous co-transfection, cell division, mitosis, metaphase, interphase, cell nucleus, nuclear structure, nuclear organization, chromatin density distribution, nuclear morphology, chromosome territories, subchromosomal domains, chromatin loop aggregates, chromatin rosettes, chromatin loops, chromatin fibre, chromatin density, persistence length, spatial distance measurement, histones, H1.0, H2A, H2B, H3, H4, mH2A1.2, DNA sequence, complete sequenced genomes, molecular transport, obstructed diffusion, anomalous diffusion, percolation, long-range correlations, fractal analysis, scaling analysis, exact yard-stick dimension, box-counting dimension, lacunarity dimension, local nuclear dimension, nuclear diffuseness, parallel super computing, grid computing, volunteer computing, Brownian Dynamics, Monte Carlo, fluorescence in situ hybridization, confocal laser scanning microscopy, fluorescence correlation spectroscopy, super resolution microscopy, spatial precision distance microscopy, autofluorescent proteins, CFP, GFP, YFP, DsRed, fusionprotein, in vivo labelling.

Literature References

Knoch, T. A. Dreidimensionale Organisation von Chromosomen-Domänen in Simulation und Experiment. (Three-dimensional organization of chromosome domains in simulation and experiment.) *Diploma Thesis*, Faculty for Physics and Astronomy, Ruperto-Carola University, Heidelberg, Germany, 1998, and TAK Press, Tobias A. Knoch, Mannheim, Germany, ISBN 3-00-010685-5 and ISBN 978-3-00-010685-9 (soft cover, 2nd ed.), ISBN 3-00-035857-9 and ISBN 978-3-00-035857-0 (hard cover, 2nd ed.), ISBN 3-00-035858-7, and ISBN 978-3-00-035858-6 (DVD, 2nd ed.), 1998.

Knoch, T. A., Münkel, C. & Langowski, J. Three-dimensional organization of chromosome territories and the human cell nucleus - about the structure of a self replicating nano fabrication site. *Foresight Institute - Article Archive*, Foresight Institute, Palo Alto, CA, USA, <http://www.foresight.org>, 1- 6, 1998.

Knoch, T. A., Münkel, C. & Langowski, J. Three-Dimensional Organization of Chromosome Territories and the Human Interphase Nucleus. *High Performance Scientific Supercomputing*, editor Wilfried Jüling, Scientific Supercomputing Center (SSC) Karlsruhe, University of Karlsruhe (TH), 27- 29, 1999.

Knoch, T. A., Münkel, C. & Langowski, J. Three-dimensional organization of chromosome territories in the human interphase nucleus. *High Performance Computing in Science and Engineering 1999*, editors Krause, E. & Jäger, W., High-Performance Computing Center (HLRS) Stuttgart, University of Stuttgart, Springer Berlin-Heidelberg-New York, ISBN 3-540-66504-8, 229-238, 2000.

Bestvater, F., **Knoch, T. A.**, Langowski, J. & Spiess, E. GFP-Walking: Artificial construct conversions caused by simultaneous cotransfection. *BioTechniques* 32(4), 844-854, 2002.